A Numerical Model of the Flow Past a Spherical-Cap Bubble Rising in a Fluidized Bed

Hendrik W. Hoogstraten[†] and Wilhard B. Rass

Department of Mathematics, University of Groningen, P.O. Box 800, 9700 AV Groningen, The Netherlands

Gertjan P. Hartholt[‡] and Alex C. Hoffmann*

Department of Chemical Engineering, University of Groningen, Nijenborgh 4, 9747 AG Groningen, The Netherlands

The shape and motion of gas bubbles in a fluidized bed are investigated by considering a single spherical-cap bubble rising vertically with free slip at its surface in an incompressible Newtonian fluid. The bubble shape, its terminal rise velocity, and the flow pattern around the bubble have been computed numerically by use of a finite element package solving the Navier−Stokes flow equations. Comparison with experimental findings shows that the bubble shape and the wake fraction can be predicted satisfactorily for a range of bubble sizes by assuming that the fluidized bed behaves as a Newtonian fluid. However, a clear-cut discrepancy was found in the terminal rise velocity. The results indicate that this discrepancy cannot be fully explained from the *a priori* assumption of the spherical-cap bubble shape, but that, most probably, some non-Newtonian fluid behavior must be invoked.

Introduction

Gas−solid fluidization is a technique by which a bed of particles within a vessel obtains liquid-like properties by a gas flow moving upward through the bed. If the gas flow is sufficiently strong, gas bubbles rise through the fluidized bed, which then looks very much like a boiling liquid. Fluidized beds are commonly used in industry both for physical and chemical processes, such as drying, granulation, catalytic cracking, and coal gasification.

The performance of processes carried out in fluidized particle beds operated in the bubbling regime is largely determined by the fluidization bubbles. The quality of the gas−solid contacting, the heat transfer within the bed and the particle mixing are all strongly dependent on the dynamics of the bubble phase (Yates, 1983). More specifically, the gas−solid contacting depends on the size and terminal velocity of fluidization bubbles. The heat transfer in the bed is dependent on the disturbance of the bulk solids (often referred to as the "dense phase") by the moving bubble phase. The main source of vertical particle mixing in the bed is the material carried upward in the wake of fluidization bubbles, while the segregation of heavier and/or larger particles toward the bottom of the bed depends on the disturbance of the dense phase by the bubble phase (Rowe and Partridge, 1962; Gibilaro and Rowe, 1974; Hoffmann and Paarhuis, 1990; Hartholt *et al.*, 1996).

It is, therefore, important to know the dynamics of fluidization bubbles in terms of the flow pattern of bulk solids around them, the terminal rise velocity, and the shape, particularly the size of the wake.

Grace (1970) investigated the rheology of the dense phase of fluidized beds on the basis of the shape of fluidization bubbles and Murray (1967) and Hoffmann *et al.* (1994) on the basis of terminal velocities. The nature of fluidized particles and fluidization bubbles has been discussed extensively in the scientific literature (see, for instance, Collins (1965, 1989) and Clift and Rafailidis (1993).

In this paper we explore how information can be gained from modeling fluidization bubbles as spherical-cap bubbles moving with free slip at their surface through a Newtonian liquid in the absence of surface tension effects. We will concentrate on the bubble shape and wake fraction with a view to improving the prediction of vertical particle mixing in batch and continuous fluidized beds. We will also look at the flow pattern around the bubbles and their terminal rise velocities. Computational techniques were used to carry out this investigation. The work builds on earlier work investigating the dynamics of spherical bubbles (Hartholt *et al.*, 1994) and spherical-cap bubbles (Hoffmann and Van den Boogaard, 1995) in liquids.

Theory and Numerical Technique

To model the rising of a gas bubble in a fluidized bed, we will consider a single spherical-cap bubble rising vertically (with its terminal velocity) along the axis of a cylindrical tube filled with an incompressible Newtonian liquid. The geometry of this flow problem is axially symmetric. The assumption of axial symmetry is reasonable for bubble Reynolds numbers less than about 100 (Clift *et al.*, 1978); the highest value encountered in this work was about 20. With respect to cylindrical coordinates (r,z) fixed to the bubble, the liquid far from the bubble flows downward with a uniform velocity U equal to the terminal rise velocity of the bubble (see Figure 1a). The bubble is bounded by two spherical surfaces: one with radius R_f (the frontal radius) and

* Author to whom correspondence should be addressed. Phone: + 31 50 3634465. Fax: + 31 50 3634479. E-mail: A.C.Hoffmann@chem.rug.nl.

[†] Phone: + 31 50 3633992. Fax: + 31 50 3633976. E-mail: H.W.Hoogstraten@math.rug.nl.

[‡] Present address: N.V. Organon, Molenstraat 110, 5340 BH Oss, The Netherlands.

S0888-5885(97)00359-X CCC: $15.00
Published on Web 01/05/1998

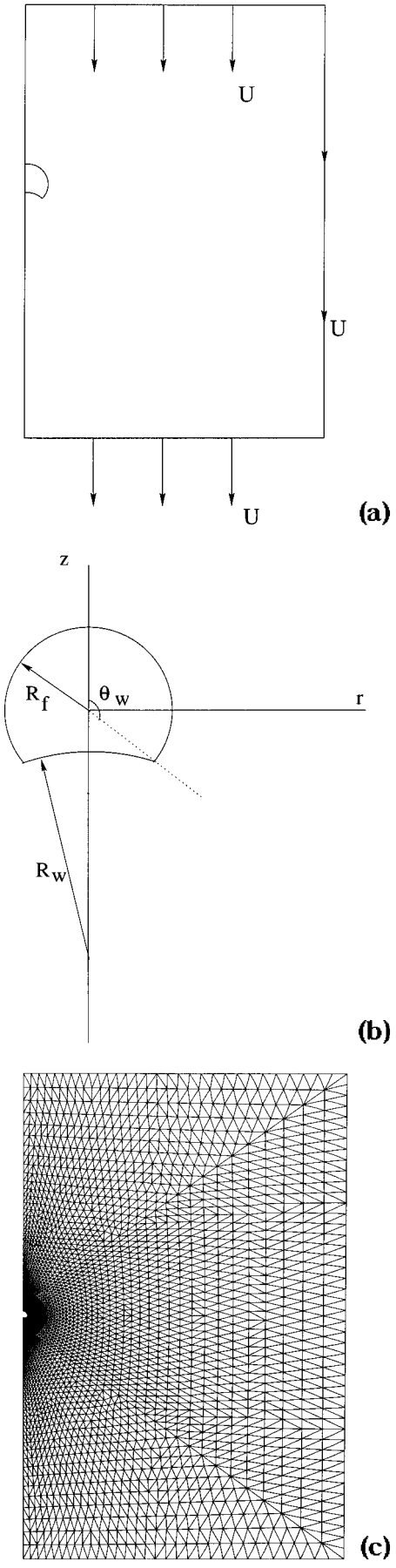

Figure 1. Flow problem (a), bubble geometry (b), and finite element grid (c).

the other with radius R_w (the wake radius). For the range of bubble sizes to be considered in this paper it has been found experimentally (Hoffmann, 1983) that the ratio of the radii R_w and R_f is (approximately) constant: $R_w/R_f \cong 2.3$, and we shall adopt this relation throughout our work. This means that the bubble shape is determined by prescribing R_f and the wake angle θ_w (see Figure 1b).

The flow problem, which is governed by the axially-symmetric Navier−Stokes equations, has been solved by use of the finite-element package SEPRAN which is based on a Galerkin discretization approach coupled with a penalty-function method to eliminate the pressure (Cuvelier *et al.*, 1986). An example of a finite-element mesh used for the present computations is shown in Figure 1c. On the cylindrical vessel wall a uniform vertical velocity U was prescribed (corresponding to the usual no-slip conditions). In all computations the vertical size of the flow domain was taken at least 60 times the bubble diameter, so that undisturbed flow conditions could be assumed at the upper (inflow) and lower (outflow) boundary. On the bubble surface a free-slip boundary condition is imposed; that is, the tangential stress is zero on both the front and the back surface of the bubble. Moreover, surface tension effects are absent. The bubble is assumed to be filled with a motionless gas with a density equal to that of air. Consequently, there is no interior flow problem to be solved. The computational procedure is largely similar to the one used in our earlier paper (Hartholt *et al.*, 1994) dealing with spherical bubbles, and for further details we refer to that paper.

The rise velocity U is determined by the requirement that the buoyancy force F_b acting on the bubble should be equal in magnitude to the flow force F_z in the negative z-direction. The buoyancy force F_b is given by

$$F_b = {}^1/_6\pi D_{eq}{}^3(\rho_l - \rho_g)g$$

where ρ_l and ρ_g denote, respectively, liquid and gas density, g is the acceleration of gravity, and D_{eq} is the volume-equivalent bubble diameter, that is, the diameter of a sphere with the same volume as the spherical-cap bubble. The flow force F_z follows from an integration of the z-component of the normal stress σ_n, due to the flow, over the two spherical surfaces constituting the bubble boundary, analogous to the case of a completely spherical bubble.

The wake angle θ_w will be determined from the requirement that the normal stress σ_n acting on the frontal bubble surface should be approximately constant. As explained by Hoffmann and Van den Boogaard (1995), this requirement follows from the continuity of σ_n across the bubble surface combined with the fact that on the gas side of this surface the viscous contribution to σ_n is negligible whereas the pressure contribution is approximately constant on that side.

The computational procedure for the flow around a bubble with given frontal radius R_f can now be summarized as follows. First, for a given value of the wake angle θ_w, the flow problem was solved for a number of values of U until that value of U was found for which the flow force F_z equalled the buoyancy force F_b. In an outer iteration loop, this computation was repeated for a sequence of θ_w-values in the expected range (with a stepsize of 10°) and the θ_w yielding the largest region of constant normal stress extending from the axis of

symmetry along the bubble front was selected by visual inspection of the profile set.

This double-nested iteration loop is an elegant way of estimating both the bubble shape and rise velocity without having to solve the full free-streamline problem. It leads to great economy in computational effort and avoids numerous sources of error arising in more complex situations. Simulations of gas bubbles in water using this technique were extensively compared with experimental data in the literature by Hoffmann and Van den Boogaard (1995) and shown to agree both in terms of bubble shape, rise velocity, and flow pattern around the bubble with a high degree of accuracy over a wide range of Reynolds numbers.

Numerical results for the case of a bubble rising in an unbounded liquid were obtained by taking the cylinder radius equal to $80R_f$, in order to eliminate any wall effects (Hartholt *et al.*, 1994). This case will henceforth be referred to as the "unbounded" case. Furthermore, simulations were performed for a cylinder diameter of 0.127 m to compare with experimental results by Hoffmann *et al.* (1994). By means of an X-ray technique, they obtained data from a rectangular fluidized bed of cross-sectional dimensions 0.127×0.178 m^2, using three powders of Geldart's group B type: two alumina catalysts and a silicon−carbide powder. In this case wall effects cannot be neglected and we will refer to it as the "bounded" case.

Since we are applying this work to the specific area of fluidized beds, and comparing our simulations with a specific experimental setup, we will present our results in terms of the parameters normally used in the fluidization literature: the bubble wake fraction and absolute values for the apparent viscosity, bubble size, and rise velocity. Reporting all our results in terms of dimensionless parameters may impede the direct comparison of this work with the fluidization literature and the application of it to fluidized-bed technology.

Results

The physical parameters of the fluid were chosen as follows: the fluid density ρ_l was set to 708.5 kg m^{-3}, the gas density ρ_g to 1.2 kg m^{-3}, and the viscosity μ was taken to lie in the range 0.3−1.0 Pa s. The fluid density ρ_l matches approximately the bulk density of the fluidized bed investigated experimentally by Hoffmann (1983) (see also Hoffmann *et al.* (1994)). The viscosity range reflects the range of experimentally determined Newtonian viscosity coefficients most often reported in the literature for fluidized particles. The frontal bubble diameters, $D_f(=2R_f)$, are in the range from 1 to 5 cm.

Bubble Shape. Figure 2 shows a typical example of the influence of the wake angle on the dimensionless normal stress profile for a constant frontal bubble diameter. The spikes seen at the edge of the bubble front originate from the flow singularity due to the assumed sharp angle at the transition from bubble front to bubble wake (see Figure 1b). For our low-Reynolds-number flows it is a very weak singularity, having a very small influence on the integration of the normal stress, needed for determining the flow force. For a bubble with $D_f = 1.68$ cm (in the bounded case with $\mu = 0.8$ Pa s) the normal stress profile is the flattest if the wake angle is 130°. The corresponding terminal rise velocity U is found to be 0.108 m s^{-1}.

With the help of the condition of near-constant stress over the bubble front surface the wake angle for bubbles

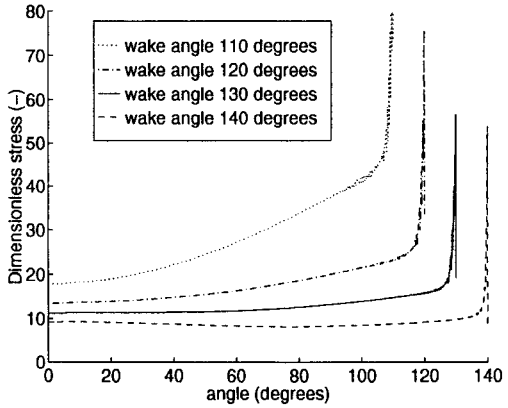

Figure 2. Normal stress profiles along the bubble front for $D_f = 1.68$ cm and various values of the wake angle θ_w in the bounded case with $\mu = 0.8$ Pa s.

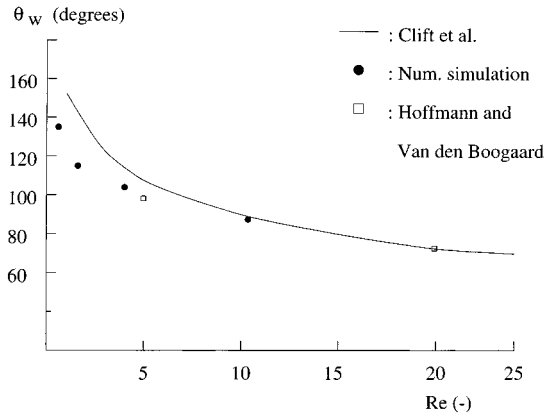

Figure 3. Wake angle θ_w as a function of the Reynolds number Re in the unbounded case.

rising in an infinite region has been determined. For several values (between 1 and 20) of the Reynolds number Re,

$$Re = \frac{\rho D_{eq} U}{\mu}$$

these numerical results are plotted in Figure 3 together with the empirical relation of Clift *et al.* (1978) for spherical-cap bubbles in liquid media:

$$\theta_w = 50 + 190 \exp(-0.62 Re^{0.4}) \qquad (Re > 1.2) \qquad (1)$$

This relation fits numerous experimental data in liquids very well. Figure 3 also contains two data points from Hoffmann and Van den Boogaard (1995) taken from their study of the steady rise of spherical-cap bubbles at intermediate Reynolds numbers in unbounded liquid media.

For bubbles with frontal diameter 0.025 m or larger (corresponding to Reynolds number values 10 and larger), the numerical results fit the experimental results well. The results of Hoffmann and Van den Boogaard computed in previous research (which was not aimed at fluidization and was concentrated on higher Reynolds numbers) agree very well with our simulations. There is, however, some discrepancy between Clift's relation (1) and the simulations in the range of smaller Reynolds numbers. This discrepancy can have different causes. On the one hand, the experimental values may be disturbed by nonidealities (e.g., surface tension affecting the bubble shape or wall effects). On

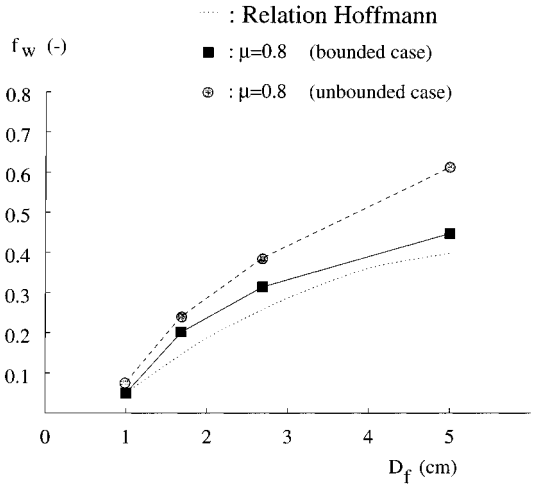

Figure 4. Wake fraction f_w as a function of bubble front diameter D_f.

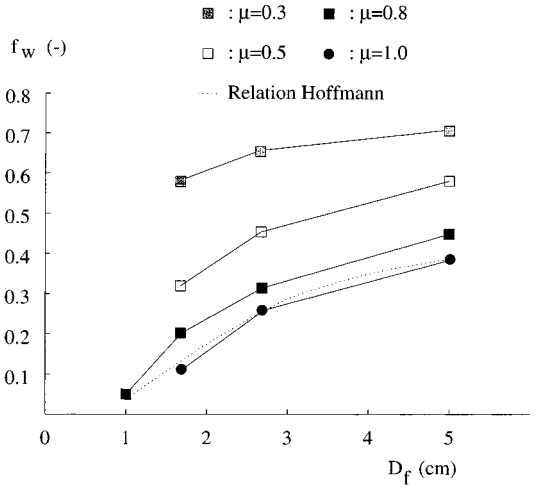

Figure 5. Wake fraction f_w as a function of bubble front diameter D_f for various values of fluid viscosity μ (Pa s) in the bounded case.

the other hand the numerical values may not be entirely accurate, since the spherical-cap shape is not ideal in the sense of giving a constant σ_n over the entire bubble front.

Hoffmann *et al.* (1993) determined an experimental relation between the frontal bubble diameter D_f (m) and the wake angle θ_w (deg) in the rectangular fluidized bed referred to earlier:

$$\theta_w = 100 + 80 \exp(-60 D_f) \qquad (2)$$

This relation is valid for bubble diameters in the range from 1.5 to 5 cm. Assuming that the wake is sphere completing, the wake fraction f_w can be calculated for a given wake angle as 1 minus the quotient of the bubble volume and the volume of a complete sphere with radius R_f. In Figure 4 the wake fraction f_w based on wake angle values obtained from eq 2 is shown together with results of our computations for both the bounded and the unbounded case. The value 0.8 Pa s, used for the fluid viscosity coefficient μ in these computations, is considered to be a reasonable estimate (Murray, 1967; Hoffmann *et al.*, 1994).

Figure 4 shows that the simulations in a column of infinite dimensions give wake fractions considerably higher than those from eq 2, as might be expected. Although the results of the numerical simulations for the bounded case do not match Hoffmann's curve exactly, they lie on a slightly higher curve with the same curvature. In order to ascertain what the effect of the assumed dense phase viscosity is on the bubble wake fraction, and whether numerical and experimental wake fractions can be brought in line, the viscosity was varied.

In Figure 5 Hoffmann's curve is plotted together with numerical results for the bounded case with viscosities of 0.3, 0.5, 0.8, and 1.0 Pa s.

From this figure it is clear that simulations in a bounded column and a viscosity of 1.0 Pa s give results that fit the relation of Hoffmann satisfactorily. The shape of these fluidization bubbles can thus satisfactorily be simulated throughout the entire size range using the *same* Newtonian viscosity of 1.0 Pa s. This is a valuable conclusion for the prediction of the wake fraction of small fluidization bubbles at formation at the gas distributor plate supporting the fluidized bed, which is to be used for the prediction of particle mixing. Although for a given powder one and the same value for the viscosity coefficient can thus be used to simulate bubble shapes, the research literature shows that the value of the apparent viscosity may well differ between powders, varying both with the particle shape and size.

As mentioned above, the calculation of the wake fraction f_w is based on the assumption of a sphere-completing wake under the spherical-cap bubble. Figure 6 shows that the spherical cap together with its wake is nearly a complete sphere, which justifies our method of determining the wake fraction. It is a question whether the toroidal flow pattern seen in the wake also reflects the actual dynamics precisely (see Clift and Rafailidis (1993)).

Bubble Rise Velocity. Davies and Taylor (1950) derived an equation for computing the terminal rise velocity for spherical-cap bubbles rising in liquids. They assumed near-potential flow over the bubble front and also applied the condition that the pressure should be constant in the neighborhood of the bubble apex. They found the following relation between the rise velocity U and the frontal bubble radius R_f:

$$U = \frac{2}{3}\sqrt{gR_f} \qquad (3)$$

This relation is plotted in Figure 7, together with some numerical results for both the bounded and the unbounded case (with $\mu = 0.8$ Pa s).

From Figure 7 it can be seen that the trend in the relation of Davies and Taylor and in the numerical results is the same. Because of the type of flow that the relation of Davies and Taylor is based on (potential flow), our numerical results will be somewhat different, particularly at low Reynolds numbers. For larger bubbles with $D_f \geq 5$ cm ($Re \geq 20$) the flow in the bed will approach potential flow and, consequently, our numerical results approach those of Davies and Taylor.

Rowe and Partridge (1965) measured the rise velocities of fluidization bubbles using an X-ray technique and found that the multiplier in eq 3 should be around 1 rather than $^2/_3$ to match their results well. Hoffmann *et al.* (1994) plotted experimentally determined bubble rise velocities against the parameter $D_f^2(1 - f_w)$. One set of their data is shown in Figure 8 together with our numerical simulations in a bounded medium with viscosity of 1.0 Pa s.

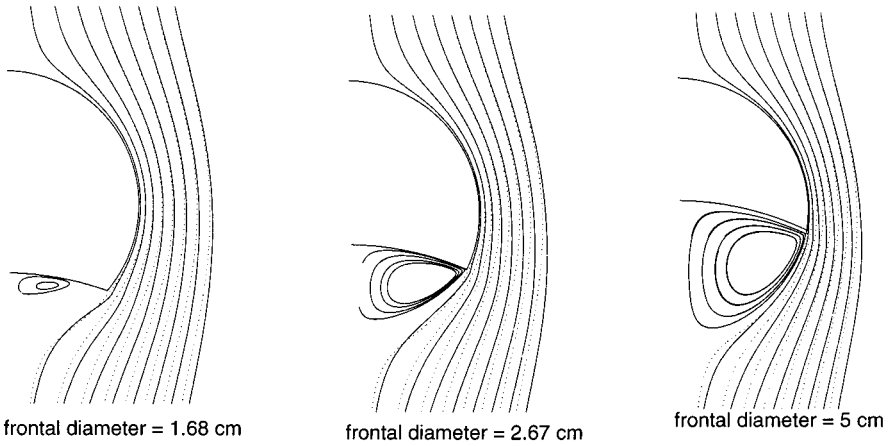

Figure 6. Comparison of flow patterns past some spherical-cap bubbles and past corresponding completely spherical bubbles in the bounded case with $\mu = 1.0$ Pa s (continuous streamlines, spherical-cap bubble; dotted streamlines, spherical bubble).

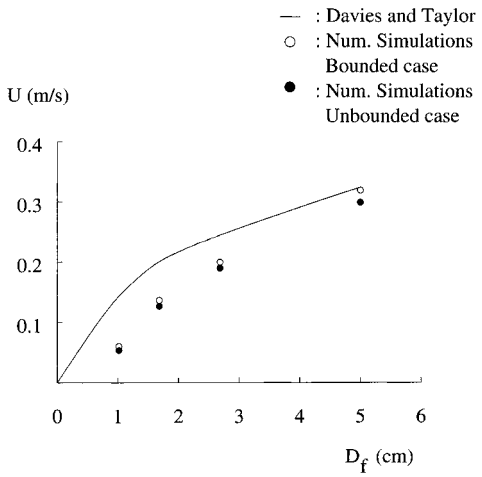

Figure 7. Terminal rise velocity U as a function of frontal diameter D_f.

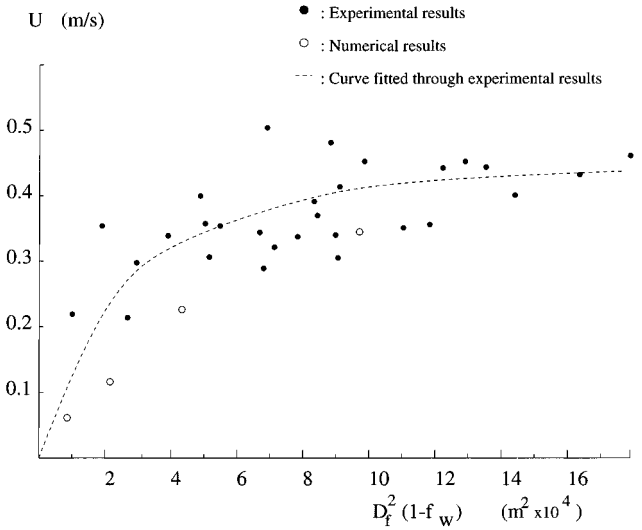

Figure 8. Terminal rise velocity U as a function of the quantity $D_f^2(1 - f_w)$.

From Figure 8, as well as from the results given by Rowe and Partridge (1965), it can be concluded that the numerical simulations lead to velocities lower than the experimental data, especially for small bubbles. Previous work (Hoffmann and Van den Boogaard, 1995) on bubbles in liquids and also the results shown in Figure 7 of this paper show that the simulations result in rise velocities approaching the Davies−Taylor velocities at higher bubble Reynolds numbers, in spite of the *a priori* assumption of a spherical-cap bubble shape. It therefore seems likely that this assumption does not, in itself, lead to very large errors in the rise velocity. It is probable that a non-Newtonian flow model must be invoked for a fully satisfactory simulation of the behavior of fluidization bubbles.

Concluding Remarks

The rising of a gas bubble in a fluidized bed has been modeled by considering a spherical-cap bubble rising with its terminal velocity in an incompressible Newtonian liquid. The flow around the bubble has been computed numerically by assuming free slip at the bubble surface and surface tension effects to be inoperative. The bubble shape has been determined on the basis of (i) a fixed ratio between frontal and wake radii and (ii) a constant normal stress acting on the bubble front. The computation of the wake fraction was based on sphere-completing flow behavior. Attention was focused on relatively small bubbles, that is, bubbles with frontal diameters from 1 to 5 cm.

The numerical predictions of the bubble shape turned out to be in agreement with experimental results for the above range of bubble sizes if a Newtonian fluid viscosity of 1.0 Pa s was chosen. The value of the apparent viscosity coefficient may vary between powders. Furthermore, the computed flow patterns confirmed the assumed sphere-completing behavior. This means that the wake fraction of the small fluidization bubbles occurring in the lowest part of the fluidized bed can be computed quite accurately, which provides useful information for the prediction of particle mixing. By contrast, the computed terminal rise velocities were found to be systematically lower than the ones observed in experiments, especially for small bubbles. The results make it likely that, for a completely satisfactory simulation of the rising of fluidization bubbles, some sort of non-Newtonian fluid behavior will be required.

List of Symbols

D = diameter, m
f = fraction
F = force, N
g = acceleration of gravity, m s^{-2}
r = radial coordinate, m
R = radius, m
Re = Reynolds number

U = terminal bubble rise velocity, m s^{-1}
z = axial (vertical) coordinate, m

Greek Symbols

μ = dynamic fluid viscosity coefficient, Pa s
ρ = density, kg m^{-3}
σ = stress, N m^{-2}
θ = angle, deg

Subscripts

b = buoyancy
eq = equivalent
f = front
g = gas
l = liquid
n = normal component
w = wake
z = axial component

Literature Cited

Clift, R.; Rafailidis, S. Interparticle Stress, Fluid Pressure, and Bubble Motion in Gas Fluidised Beds. *Chem. Eng. Sci.* **1993**, *48*, 1575−1582.

Clift, R.; Grace, J. R.; Weber, M. E. *Bubbles, Drops and Particles*; Academic Press, Inc.: London, 1978.

Collins, R. An Extension of Davidson's theory of bubbles in fluidized beds. *Chem. Eng. Sci.* **1965**, *20*, 747−755.

Collins, R. A model for the effects of voidage distribution around a fluidization bubble. *Chem. Eng. Sci.* **1989**, *44*, 1481−1487.

Cuvelier, C.; Segal, A.; Van Steenhoven, A. A. *Finite Element Methods and Navier-Stokes Equations*; D. Reidel Publishing Company: Dordrecht, 1986.

Davies, R. M.; Taylor, G. I. The Mechanics of Large Bubbles Rising through Extended Liquids and through Liquids in Tubes. *Proc. R. Soc. London* **1950**, *A200*, 375−390.

Gibilaro, L. G.; Rowe, P. N. A Model for a Segregating Gas Fluidised Bed. *Chem. Eng. Sci.* **1974**, *29*, 1403−1412.

Grace, J. R. The Viscosity of Fluidized Beds. *Can. J. Chem. Eng.* **1970**, *48*, 30−33.

Hartholt, G. P; Hoffmann, A. C.; Janssen, L. P. B. M.; Hoogstraten, H. W.; Moes, J. H. Finite Element Calculations of Flow past a Spherical Bubble Rising on the Axis of a Cylindrical Tube. *J. Appl. Math. Phys. (ZAMP)* **1994**, *45*, 733−745.

Hartholt, G. P.; Hoffmann, A. C.; Janssen, L. P. B. M. Direct Visual Observation of Individual Particles in Gas and Liquid Fluidised Beds. *Powder Technol.* **1996**, *88*, 341−345.

Hoffmann, A. C. Ph.D. Thesis, Department of Chemical and Biochemical Engineering, University College London, 1983.

Hoffmann, A. C.; Paarhuis, H. A Study of the Particle Residence Time Distribution in Vertically Moving Fluidised Beds. *IChemE Symp. Ser.* **1990**, *121*, 37−49.

Hoffmann, A. C.; Van den Boogaard, H. A. A Numerical Investigation of Bubbles Rising at Intermediate Reynolds and Large Weber Numbers. *Ind. Eng. Chem. Res.* **1995**, *34*, 366−372.

Hoffmann, A. C.; Janssen, L. P. B. M.; Prins, J. Particle Segregation in Fluidised Binary Mixtures. *Chem. Eng. Sci.* **1993**, *48*, 1583−1592.

Hoffmann, A. C.; Hartholt, G. P.; Yates, J. G. On the Rheology of the Dense Phase of a Gas Fluidised Bed. *Chem. Eng. Commun.* **1994**, *130*, 31−44.

Murray, J. D. On the Viscosity of a Fluidized System. *Rheol. Acta* **1967**, *6*, 27−30.

Rowe, P. N.; Partridge, B. A. Particle Movement Caused by Bubbles in a Fluidised Bed. In *Interaction between Fluids and Particles*; Institution of Chemical Engineers: London, 1962; pp 135−142.

Rowe, P. N.; Partridge, B. A. An X-ray Study of Bubbles in Fluidised Beds. *Trans. Inst. Chem. Eng.* **1965**, *43*, T157−T175.

Yates, J. G. *Fundamentals of Fluidized-Bed Chemical Processes*; Butterworths: London, 1983.

Received for review May 19, 1997
Revised manuscript received September 16, 1997
Accepted September 18, 1997[⊗]

IE9703595

[⊗] Abstract published in *Advance ACS Abstracts*, November 15, 1997.